PCCP

Accepted Manuscript

This is an *Accepted Manuscript*, which has been through the Royal Society of Chemistry peer review process and has been accepted for publication.

Accepted Manuscripts are published online shortly after acceptance, before technical editing, formatting and proof reading. Using this free service, authors can make their results available to the community, in citable form, before we publish the edited article. We will replace this *Accepted Manuscript* with the edited and formatted *Advance Article* as soon as it is available.

You can find more information about *Accepted Manuscripts* in the Information for Authors.

Please note that technical editing may introduce minor changes to the text and/or graphics, which may alter content. The journal's standard Terms & Conditions and the Ethical guidelines still apply. In no event shall the Royal Society of Chemistry be held responsible for any errors or omissions in this *Accepted Manuscript* or any consequences arising from the use of any information it contains.

www.rsc.org/pccp

Journal Name

ARTICLE

Effect of Co-Sensitization Sequence on the Performance of Dye-Sensitized Solar Cells with Porphyrin and Organic Dyes

Suhua Fan,[a,b] Xuefeng Lu,[a] Hong Sun,[a] Gang Zhou,[a] Yuan Jay Chang[c] and Zhong-Sheng Wang[a*]

To obtain a broad spectral response in the visible region, the TiO_2 film is co-sensitized with a porphyrin dye (FNE57 or FNE59) and an organic dye (FNE46). It is found that the stepwise co-sensitization in one single dye solution followed by in another single dye solution is better than the co-sensitization in a cocktail solution in terms of photovoltaic performance. The stepwise co-sensitization first with a porphyrin dye and then with an organic dye outperforms that in a reverse order. The DSSC devices based on co-sensitizers FNE57 + FNE46 and FNE59 + FNE46 with a quasi-solid-state gel electrolyte generate power conversion efficiency of 7.88% and 8.14%, respectively, which exhibits remarkable efficiency improvements of 61% and 35%, as compared with the device sensitized with the porphyrin dye FNE57 and FNE59, respectively. Co-sensitization brings about much improved short-circuit photocurrent due to the complementary absorption of the two sensitizers. The observed enhancement of incident monochromatic photon-to-electron conversion efficiency from individual dye sensitization to co-sensitization is attributed to the improved charge collection efficiency rather than to the light harvestinhg efficiency. Interestingly, the open-circuit photovoltage for the co-sensitization system comes between the higher voltage for the porphyrin dye (FNE57 or FNE59) and the lower voltage for the organic dye (FNE46), which is well correlated with their electron lifetimes. This finding indicates that not only the spectral complementation but also the electron lifetime should be considered to select dyes for co-sensitization.

Introduction

Dye-sensitized solar cells (DSSCs) made from mesoporous TiO_2 electrodes have drawn much attention as a promising candidate because of their high power conversion efficiencies, ease of fabrication, and low manufacturing costs.[1-3] The photosensitizers, as an important component in DSSCs, play a crucial role in getting a higher solar-to-electricity conversion efficiency. A lot of efforts have been devoted to the development of novel and efficient sensitizers, such as ruthenium complexes,[4-7] zinc porphyrins [8-12] and metal-free organic dyes, [13-17] serving as efficient light harvesters for DSSCs. DSSCs employing ruthenium (II)-based dyes have achieved power conversion efficiency (*PCE*) of > 11% so far. [4, 6, 18] However, the rare resources of ruthenium and the environmental problems may hamper their widespread applications. Thus, metal-free organic dyes and noble-metal-free porphyrins have been intensively explored owing to their ease of molecular modification and large molar extinction coefficients. [8-17]

a Department of Chemistry, Lab of Advanced Materials, Collaborative Innovation Center of Chemistry for Energy Materials, Fudan University, Shanghai 200438, P. R. China. E-mail: zs.wang@fudan.edu.cn
b School of Chemistry & Material Engineering, Fuyang Normal College, Fuyang, Anhui 236037, P. R. China.
c Department of Chemistry, Tung Hai University, NO. 1727, Sec.4, Taiwan Boulevard, Xitun District, Taichung, Taiwan 40704, P. R. China.
Electronic Supplementary Information (ESI) available: [details of any supplementary information available should be included here]. See DOI: 10.1039/x0xx00000x

Porphyrins and related derivatives have been considered to be promising candidates for DSSCs due to their intense Soret and Q bands, versatile modifications of their core, and tuneable spectral properties. The breakthrough achieved in 2011 by Michael Grätzel et al. is the PCE of 12.3% obtained from a push–pull zinc porphyrin YD2-*o*-C8 co-sensitized with an organic dye (Y123).[10] This milestone finding stimulates investigation of D-π-A porphyrin dyes in developing high-efficiency DSSCs.[11-12, 19-23] However, the drawback of the porphyrin dyes is that they display pretty weak absorption in the spectral region between Soret and Q bands. To overcome this drawback, the design of sensitizers towards broad visible light absorption into the near-infrared (NIR) region[22, 24-26] and co-sensitization[21, 27-30] with different dyes (cocktail-type) has been demonstrated to be an effective means to broaden the photoelectric response range. Among them, co-sensitization through a combination of two or more dyes having complementary absorption properties has been demonstrated to extend the spectral response range effectively. For example, the co-sensitization of two organic dyes (JK2 and SQ1) with complementary spectral responses resulted in an improved photovoltaic performance relative to those of the individual dyes; [31] co-sensitization of TiO_2 films with ruthenium dye (the black dye) and an organic dye Y1 yielded a significantly enhanced photocurrent such that the device performance attained *PCE* = 11.28%.[27] For porphyrins, a device based on co-sensitization of a TiO_2 film with XW4 and an organic dye C1 showed a short-circuit current density (J_{sc}) increase by 24% and a slight improvement of the open-circuit

photovoltage (V_{oc}) by 5%, resulting in an improved cell efficiency (10.45%).[21] However, the co-sensitization of YD2-*o*-C8 with Y123 produced an enhancement of J_{sc} from 17.3 to 18.2 mA cm^{-2} but a decrease in V_{oc} from 965 to 891 mV.[10] While the co-sensitization is extensively employed for photocurrent enhancement, its effect on V_{oc}, the cause of the voltage change, and the effect of co-sensitization sequence on solar cell performance have rarely been studied.

Recently, we have designed and synthesized three novel D-π-A Zn(II)-porphyrin sensitizers (FNE57, FNE58, and FNE59) containing the same electron donating moiety (carbazole) and the same electron-withdrawing moiety (cyanoacrylic acid).[32] The effect of the position for the incorporated auxiliary acceptor, 2,3-diphenylquinoxaline (DPQ), on the absorption properties of sensitizer and the photovoltaic performance is systematically investigated. However, the quasi-solid-state device based on the porphyrin dye FNE59 only reaps a *PCE* of 6.02%. In an effort to obtain highly efficient properties for porphyrin sensitizers, we make use of an organic dye (FNE46),[33] which has strong light response at 525 nm to complement the spectral response of porphyrin sensitized devices, to co-sensitize the TiO$_2$ film aiming at enhancing the absorption in the valley between Soret and Q bands for the porphyrin. As the quasi-solid-state gel electrolyte is much better than the volatile organic electrolyte in view of long-term stability, quasi-solid-state DSSCs have been systematically studied in this work. To understand the effect of co-sensitization sequence on solar cell performance, we have compared the stepwise co-sensitization in different order. Furthermore, the co-sensitization effect on photovoltage and the cause of voltage change have also been investigated in order to clarify the factors influencing co-sensitization effect besides the spectral complementation.

Experimental Section

Synthesis of dyes

The detailed synthetic processes of porphyrin dyes (FNE57 and FNE59) have been reported in literature.[32] Firstly, the porphyrin core was obtained using functionalized aldehyde precursors and 2,2'-dipyrromethane through acid-catalyzed condensation in dichloromethane followed by oxidation with 2,3-dichloro-5,6-dicyano-1,4-benzoquinone. Then, monoaldehyde-substituted porphyrin derivative was synthesized by Vilsmeier reaction. Zn(II)-porphyrin was prepared by metalation of free base porphyrin and zinc acetate. Finally, the desired Zn(II)-porphyrin sensitizers FNE57 and FNE59 were obtained through a Knoevenagel condensation reaction. The organic dye FNE46 was prepared according to the previous method.[33] The dye starting from 5,8-dibromoquinoxaline, was synthesized via a Stille coupling, Vilsmeier reaction, Suzuki coupling and Knoevenagel condensation. All target dyes were fully characterized by ^{1}H NMR, ^{13}C NMR spectroscopy, and mass spectroscopy.

Characterizations and measurements

UV–vis absorption spectra of the dyes were measured in THF solutions and on TiO$_2$ films with a Shimadzu UV–2550PC spectrophotometer. The time-resolved luminescence experiments were recorded on Lifespec-ps PDL 800-B (Edinburgh). The charge densities at open-circuit were performed using charge extraction method.[34] The electron lifetimes were obtained from controlled intensity modulated photovoltage spectroscopy (IMVS),[35] which was carried out on an electrochemical workstation (Zahner XPOT, Germany) equipped with a white light emitting diode (LED). The intensity-modulated spectra were scanned in a frequency range from 0.1 Hz to 10 kHz under illumination of LED light with various light intensity ranging from 20 to 120 W m^{-2}, in modulation amplitude less than 5% of the light intensity.

DSSC fabrication and photovoltaic measurements

A 15-µm thick TiO$_2$ film (active area 0.25 cm^2) was prepared with a screen-printing technique. The films were first sintered at 500 °C for 2 h and then treated with 0.05 M TiCl$_4$ aqueous solution for 30 min at 70 °C followed by calcinations at 450°C for 30 min before immersing in dye solutions. 0.2 mM porphyrin solutions containing 0.4 mM deoxycholic acid (DCA)[32] and 0.4 mM FNE46 were used in this work. TiO$_2$ films were immersed in a single dye solution or a cocktail-type dye solution for 18 h. For the stepwise co-sensitization, TiO$_2$ electrodes were first immersed in a porphyrin dye solution (0.2 mM in THF/ethanol, 3:2, v/v) with 0.4 mM DCA for 6 h, rinsed with acetonitrile, and then transferred into the FNE46 solution (0.4 mM in THF) for 12 h. For comparison, stepwise co-sensitization with opposite order was also carried out. Afterwards, the electrodes were rinsed with acetonitrile to remove the physically adsorbed dyes. The Pt counter electrode was prepared by coating drop of H$_2$PtCl$_6$ solution on an FTO plate and heating for 30 min at 400°C. A DSSCs device was fabricated with a dye-adsorbed TiO$_2$ electrode, Pt-counter electrode and a redox electrolyte. Quasi-solid-state gel electrolyte was prepared by mixing 5 wt% poly(vinylidenefluoride-co-hexafluoropropylene) in a redox solution containing 0.1 M LiI, 0.05 M I$_2$, 0.6 M 1,2-dimethyl-3-*n*-propylimidazolium iodide (DMPImI) and 0.5 M 4-*tert*-butylpyridine (TBP) in 3-methoxypropionitrile (MPN) under heating until all solids were dissolved. After introducing the hot gel solution into the internal space of the cell from the two holes predrilled on the back of the counter electrode, a uniform motionless polymer gel layer was formed between the working and the counter electrodes, and then the holes were sealed with UV curing sealant. The working performance of DSSCs was tested by recording the current density-voltage (*J-V*) curves with a Keithley 2420 source meter under illumination of simulated AM1.5G solar light coming from a solar simulator (Sol3A equipped with a 450 W Xe lamp and an AM1.5G filter, Newport). The light intensity was calibrated using a standard Si solar cell (Newport 91150). Action spectra of the incident monochromatic photon-to-electron conversion efficiency (IPCE) for the solar cells were recorded using an SM-250 system (Bunkoh-Keiki, Japan). The intensity of

monochromatic light was measured with a Si detector (S1337-1010BQ).

Results and discussion

Structures and energy levels of dyes

The structures of the porphyrin dyes (FNE57 and FNE59) and co-sensitizer (FNE46) are depicted in Scheme 1a, and the energy diagram is shown in Scheme 1b.[32, 33] The lowest unoccupied molecular orbital (LUMO) levels of the three dye molecules are more negative than the conduction band (CB, −0.50 V vs. NHE) of TiO_2 (Scheme 1b), which enables the electron injection from the excited states of the dyes to the CB of TiO_2.[36] On the other hand, the highest occupied molecular orbital (HOMO) levels of the three dyes are more positive than the redox potential of I^-/I_3^- redox couple (0.40 V vs. NHE, Scheme 1b), indicating that the oxidized dyes generated by the electron injection process can thermodynamically accept electrons from I^- ions to regenerate the oxidized dye molecules.
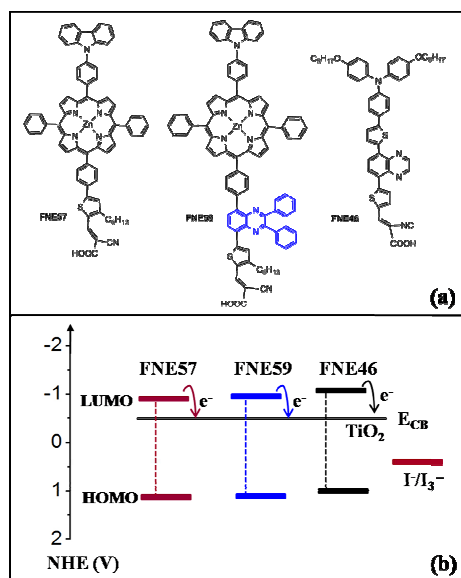
Scheme 1 (a) The molecular structures of FNE57, FNE59, and FNE46 dyes and (b) schematic diagram of energy levels (vs. NHE) of TiO_2 conduction band, dyes, and I^-/I_3^- redox couple.

Optical properties

Fig.1 shows the absorption spectra of FNE57, FNE59, and FNE46 in THF solution and on TiO_2 films, respectively. The porphyrin FNE57 in a THF solution shows a strong absorption peak centered at 427 nm and two weak absorption peaks at 557 and 598 nm, which respectively correspond to the Soret and Q bands of porphyrin-based dye molecules.[32] For FNE59, the Soret band is located at 425 nm, and the Q bands are located at 557 and 597 nm. The FNE46 presents strong absorption between 460 and 540 nm in THF solution (Fig. 1a),[33] where the absorption for the porphyrins is very weak.

The complementary absorption of FNE46 and the porphyrins is crucial to co-sensitization.[37]

Fig. 1b presents the absorption spectra of individual dye and co-sensitizer anchored TiO_2 films on transparent conducting glass. When the individual dye molecule was attached onto the nanocrystalline TiO_2 surface, similar absorption features to the corresponding dye solutions were observed for sensitizers FNE57 and FNE59. However, a hypochromic shift of 25 nm was observed for sensitizer FNE46, which is attributed to the H-type aggregation of the FNE46 on the TiO_2 surface.[38] The co-adsorbed TiO_2 film with FNE57 + FNE46 and FNE59 + FNE46 exhibited enhanced light absorption as compared with the individual dye loaded films. Notably, the absorption around Q band was obviously broadened in comparison to the absorption characteristics in solution. Moreover, the ratio of intensities at 558 and 430 nm was increased from 0.1 (FNE57 and FNE59) to 0.5 (FNE57 + FNE46 and FNE59 + FNE46), respectively, indicating that the absorption around Q bands was strengthened significantly by co-sensitization of FNE46. And the ratio of intensities at 430 and 493 nm was increased from 0.77 for FNE46 to 1.19 for FNE57 + FNE46 and 1.37 for FNE59 + FNE46, respectively, indicating that the absorption near 430 nm for FNE46 was also complemented by the Soret band of porphyrin dyes. The broad and strong spectral coverage from 400 to 700 nm achieved with the co-sensitization of FNE57 + FNE46 and FNE59 + FNE46 exhibits a panchromatic sunlight harvesting to enhance the light-harvesting efficiency (LHE).
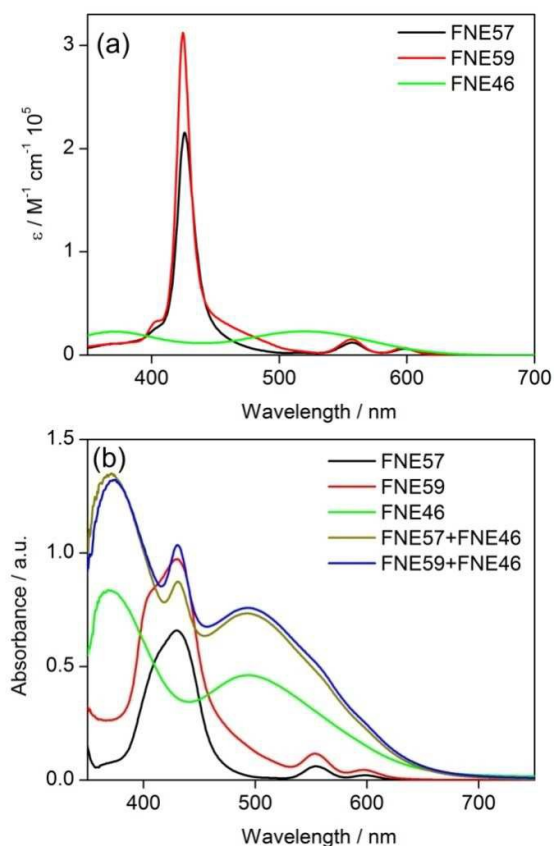
Fig. 1 Absorption spectra of (a) FNE57, FNE59, and FNE46 in THF solution ($c = 8.0 \times 10^{-6}$ mol/L) and (b) FNE57, FNE59, FNE46, FNE57 + FNE46, and FNE59 + FNE46 on 2.5 μm TiO$_2$ films.

Photovoltaic performance of DSSCs

The quasi solid- state DSSCs co-sensitized by FNE57 (or FNE59) with FNE46 on TiO$_2$ films of thickness 15 μm were achieved via a stepwise approach: the TiO$_2$ electrode was firstly immersed in the FNE57 (or FNE59) solution for 6 h and then immersed in the FNE46 solution for 12 h. Afterwards, the co-sensitized film was assembled into a DSSC device with a Pt-coated counter electrode and filled with a quasi-solid-state gel electrolyte. Fig. 2 shows IPCE action spectra as a function of the light wavelength and the photocurrent density-voltage (*J-V*) characteristics for the individual dye or co-sensitizers based devices under standard test conditions, and the corresponding photovoltaic parameters are summarized in Table 1. It can be found that the IPCE spectra of individual FNE57, FNE59, and FNE46 display typical characteristics of the electronic absorption of the sensitized TiO$_2$ layer.[32, 33] After co-sensitization, the IPCE spectra of FNE57 + FNE46 and FNE59 + FNE46 became broader with high IPCE values between 400 and 650 nm, and the tail extended to 800 nm.

The IPCE is determined by the light-harvesting efficiency (LHE), the quantum yield of electron injection (Φ_{inj}), and the collection efficiency of the photo-generated charge carriers (Φ_{coll}), as shown in the following equation:[4]

$$IPCE(\lambda) = LHE(\lambda) \times \Phi_{inj} \times \Phi_{coll} \qquad (1)$$

These different factors will be clarified separately to find out the reasons for the much higher IPCE values obtained with co-sensitizers as compared to those obtained with the single dye. Here, as all the single dyes have similar HOMO and LUMO energy levels, the Φ_{inj} should be similar for the three individual dyes and their mixtures. As the absorbance at the Soret band for FNE57 and FNE59 and the absorbance at 495 nm for FNE46 loaded 2.5 μm thick TiO$_2$ films are 0.73, 0.95, and 0.47, respectively, the LHE for the 15 μm dye-loaded TiO$_2$ film is close to unity for all these films. Owing to the similar LHE and Φ_{inj}, the IPCE enhancement from individual dye sensitization to co-sensitization should be attributed to the improved charge collection efficiency.
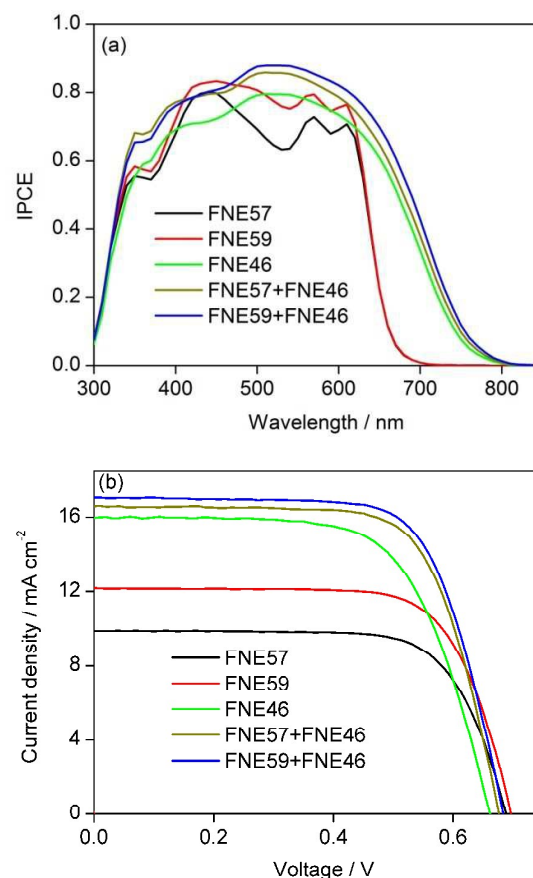
Fig. 2 (a) The IPCE action spectra and (b) current-voltage curves for DSSCs based on FNE57, FNE59, FNE46, FNE57 + FNE46, and FNE59 + FNE46 with a quasi-solid-state gel electrolyte.

To further unravel the possible difference of injection efficiency between the individual dye and co-sensitizers, time-resolved luminescence experiments were performed. Fig. S1 in the ESI† presents the time-resolved luminescence of the three individual dyes in THF solutions and adsorbed on 2.5 μm TiO$_2$ films. The fluorescence lifetimes for FNE57, FNE59, and FNE46 in THF solutions were 1.08, 0.96, and 0.45 ns, respectively. The fluorescence of FNE57 and FNE59 decayed more rapidly than the organic dye FNE46. The fluorescence decay was further enhanced for co-sensitizers FNE57 + FNE46 and FNE59 + FNE46 adsorbed on TiO$_2$ film. The rapid quenching of luminescence suggests unity charge injection from the excited state of the dye into the conduction band of TiO$_2$.[10, 39]

The photovoltaic results display a clear trend with the *PCE* for the single-dye sensitized devices in the following order: FNE46 (*PCE* = 6.87%) > FNE59 (*PCE* = 6.02%) > FNE57 (*PCE* = 4.90%). Upon co-sensitization, the quasi-solid-state DSSCs based on sensitizers FNE57 + FNE46 and FNE59 + FNE46 gave improved DSSC performance, which achieved J_{sc} of 16.59 and 17.03 mA cm^{-2}, V_{oc} of 676 and 683 mV, and fill factor (*FF*) of 0.70, corresponding to *PCE* of 7.88 and 8.14%. The J_{sc} value of the DSSC with co-sensitizers sensitized devices is 61% and 35% higher than that of FNE57 and FNE59, respectively, as weak Q bands of porphyrins are strengthened by the absorption of

FNE46. Owing to the significant improvement of the J_{sc}, the *PCE* is enhanced notably upon co-sensitization.

Table 1. Photovoltaic parameters of the cocktail-type quasi-solid-state DSSCs based on sensitizers FNE57, FNE59, FNE46, FNE57 + FNE46, and FNE59 + FNE46.

Devices	V_{oc}/mV	J_{sc}/mA cm^{-2}	FF	PCE/%
18h in FNE57	689±3	9.88±0.29	0.72±0.01	4.90±0.08[32]
18h in FNE59	703±8	12.06±0.22	0.71±0.01	6.02±0.12[32]
18h in FNE46	661±3	15.99±0.21	0.65±0.02	6.8±0.05
6h in FNE57 + 12h in FNE46	676±5	16.59±0.35	0.70±0.01	7.88±0.19
A (6h in FNE59 + 12h in FNE46)	683±4	17.03±0.27	0.70±0.02	8.14±0.09
B (12h in FNE46 + 6h in FNE59)	678±6	16.60±0.31	0.70±0.01	7.88±0.13
C [18h in (FNE46 + FNE59)]	671±6	16.32±0.35	0.69±0.01	7.56±0.11

To study the effect of dye loading sequence on the device performance, we investigated the soaking process of FNE59 and FNE46 dyes, and the results are summarized in Table 1. The anode TiO$_2$ film sensitized first with FNE59 (6 h) and then with FNE46 (12 h) (denoted as A) gave the best *PCE* of 8.14%. When a reversed soaking process was applied, the device (denoted as B) obtained a *PCE* of 7.88%. When the anode film was immersed in a cocktail dye solution of FNE46 + FNE59, the efficiency depended on the molar ratio of the two dyes. The molar ratio between co-sensitizers FNE59 and FNE46 was optimized for a cocktail-type quasi-solid-state DSSC, and the photovoltaic data is summarized in Table S2. As seen in Table S2, FNE46 and FNE59 co-sensitized device with a molar ratio of 3.5:1 (denoted as C, Table 1) achieved the best efficiency of 7.56%.

The efficiency increases in the order of C, B, A, which is consistent with the J_{sc} order of C (16.32 mA cm^{-2}) < B (16.60 mA cm^{-2}) < A (17.03 mA cm^{-2}). The photocurrent order is confirmed by the IPCE spectra shown in Fig. S2, where the IPCE values in the visible region increase in the order of C < B < A (see ESI†). To understand the photocurrent differences from a chemistry perspective, the quantity of the dyes adsorbed on TiO$_2$ was estimated by desorbing the dyes from the TiO$_2$ film into a 0.01 M Bu$_4$NOH-THF solution. Table S3 lists the dye-loading densities calculated from the absorption spectra of the resultant solutions (see ESI†). The adsorbed amount of porphyrin in film B (1.96 × 10^{-8} mol cm^{-2}) is lower than that in film A (2.77 × 10^{-8} mol cm^{-2}) by 29% while the loading amount of FNE46 is similar in both films, indicating that first loading of the FNE46 dye may inhibit further adsorption of the bulky porphyrin while first loading of the bulky porphyrin does not influence the adsorption of FNE46 with smaller size. Therefore, device A produced higher J_{sc} than device B. Compared with A and B, the lower photocurrent of C is attributable to its smaller amount of dye adsorption on the TiO$_2$ film. The above results suggested that the incubation of FNE59-adsorbed film in FNE46 solution is the most appropriate method in our research.

It is noted that the V_{oc} is different for these devices. The V_{oc}/mV displays a systematic trend for devices in the order of FNE59 (703) > FNE57 (689) > FNE59 + FNE46 (683) > FNE57 + FNE46 (676) > FNE46 (661). The V_{oc} of a DSSC device is determined by the conduction band edge and the recombination of photo-injected electrons in TiO$_2$ film with either electron accepting species in electrolytes or dye cations. [40] To understand the difference of V_{oc} for these devices, the relative conduction band edge positions and electron lifetimes in the DSSCs were investigated by means of charge extraction technique and intensity modulated photovoltage spectroscopy (IMVS) measurement. Fig. 3 shows plot of V_{oc} *vs*. Q for the single dye-sensitized and co-sensitized systems at seven intensities of white light from a LED lamp. In general, DSSCs sensitized with the individual dye or co-sensitizers feature a similar extracted charge (Q) at the same potential bias V_{oc}, suggesting a similar conduction band edge of TiO$_2$ for these devices. Therefore, the different V_{oc} value observed for these quasi-solid-state DSSCs should be ascribed to the different charge recombination kinetics.
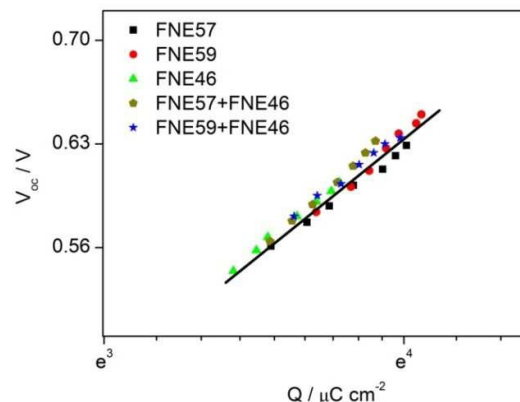
Fig. 3 Charge density at open circuit as a function of V_{oc} for DSSCs with FNE57, FNE59, FNE46, FNE57 + FNE46, and FNE59 + FNE46.

Fig. 4 shows the electron lifetime as a function of the charge density for these quasi-solid-state DSSCs. The electron lifetime was measured by IMVS and obtained from the frequency at the top of the semicircle (f_{min}) according to equation (2): [41, 42]

$$\tau = (2\pi f_{min})^{-1} \qquad (2)$$

As shown in Fig. 4, the porphyrin dye exhibits higher electron lifetime than the organic dye. This is due to the bulky structure of the porphyrin, which is more effective to block charge recombination between electrons and I$_3^-$ ions. As FNE59 is more bulky than FNE57, it is reasonable that the former gives longer electron lifetime than the latter.[32] The co-sensitized system comes between the individual dyes in electron lifetime, which is the result that the porphyrin has stronger suppressing ability of charge recombination than FNE46. The electron lifetime decreases in the order of FNE59 > FNE57 > FNE59 + FNE46 > FNE57 + FNE46 > FNE46 at a given charge Q, which is consistent with the trend of variation of V_{oc}. Therefore, the different V_{oc} values can be explained by their

different electron lifetimes because these photoanodes have similar CB edges.

Co-sensitization has been extensively studied using porphyrin dyes and metal-free organic dyes.[43-45] While the J_{sc} enhancement was achieved, the V_{oc} sometimes increased and sometimes decreased, depending on the co-sensitization system. This was attributed to the collective effect of shifted conduction band and changed charge recombination rate, as revealed by Diau et al.[44,45] In our system, as the conduction band does not shift, the V_{oc} is well correlated with the electron lifetime. The experimental results suggest that not only the spectral complementation but also the electron lifetime should be considered to select dyes for co-sensitization. For future research work on co-sensitization, one should first select dyes having good spectral complementation, and then study the kinetics of charge recombination. Those dyes possessing both good spectral complementation and same or similar electron lifetime should be selected for co-sensitization. This not only can improve J_{sc} significantly, but also can avoid voltage loss.
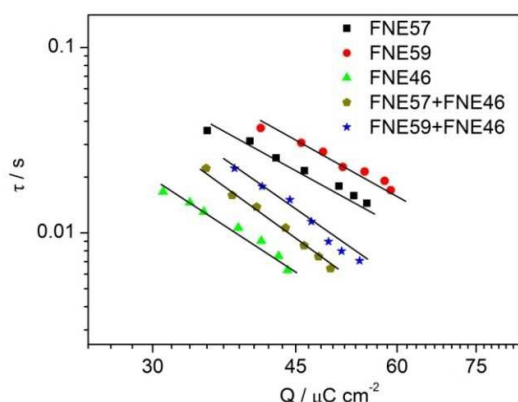
Fig. 4 Electron lifetime as a function of charge density at open-circuit photovoltage for DSSCs based on FNE57, FNE59, FNE46, FNE57 + FNE46, and FNE59 + FNE46.
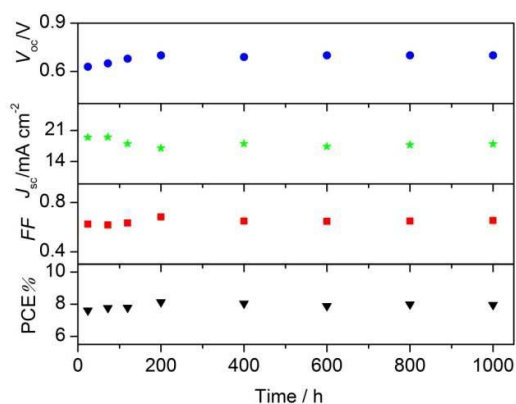
Fig. 5 A test of stability of devices over 1000 h showing the variations of photovoltaic parameters (J_{sc}, V_{oc}, FF, and PCE) for FNE59 + FNE46 co-sensitized DSSC based on quasi-solid-state electrolyte under one sun soaking.

For the future practical applications, it is of importance for the DSSC devices to achieve a long lifetime. Since quasi-solid-state gel electrolytes are non-flowing and non-volatile, the

corresponding quasi-solid-state DSSCs have shown good stability. We tested the stability for the FNE59 + FNE46 co-sensitized quasi-solid-state DSSCs under one sun soaking for a period of 1000 h. Fig. 5 shows the temporal variations of J_{sc}, V_{oc}, FF, and PCE for the system. V_{oc}, FF, and PCE values increased initially followed by a plateau, while J_{sc} values faintly decreased at the beginning and then remained almost constant. For example, the device attained the PCE from 7.62% to 7.79% during the period of 24–120 h; the efficiency then increased to 8.14% at 200 h. After 200 h, the performance of the co-sensitized device remained stable until the end of the test (1000 h). The overall efficiency changed within 7% of the initial value during 1000 h of one sun soaking, which indicates that the quasi-solid-state DSSC based on co-sensitizers FNE59 + FNE46 demonstrates good long-term stability during light soaking.

Conclusions

In summary, porphyrin dyes show obviously enhanced photovoltaic performance for the quasi-solid-state DSSCs when co-sensitized with an organic dye that has a complementary spectral response. The co-sensitization approach significantly enhanced the J_{sc} value and broadened the IPCE response. Thus, the best cell gives J_{sc} = 17.03 mA cm^{-2}, V_{oc} = 683 mV, FF = 0.70, and PCE = 8.14% under standard AM1.5G one-sun irradiation, which exhibits remarkable overall efficiency improvement of 35% as compared with the device individually sensitized by the porphyrin dye FNE59. The co-sensitized devices also exhibit good long-term stability after continuous light soaking for 1000 h. The photovoltaic performances of single-dye and co-sensitized systems are related to the absorption properties of the dye loaded TiO_2 film and the charge recombination rate for the device. The enhanced J_{sc} of co-sensitized systems is due to the combined light-harvesting effect of two dyes that have complementary absorption range. The change of V_{oc} is well correlated with the electron lifetime. To get a high photovoltage for the co-sensitized system, same or similar electron lifetime of the used dyes should also be considered in addition to the spectral complementation.

Acknowledgements

References

1   B. O'Regan and M. Grätzel, *Nature*, 1991, **353**, 737–740.
2   M. Grätzel, *Acc. Chem. Res*., 2009, **42**, 1788–1798.

3   A. Hagfeldt, G. Boschloo, L. Sun, L. Kloo and H. Pettersson, *Chem. Rev.*, 2010, **110**, 6595–6663.

4   M. K. Nazeeruddin, A. Kay, I. Rodicio, R. Humphry-Baker, E. Mueller, P. Liska, N. Vlachopoulos and M. Grätzel, *J. Am. Chem. Soc.*, 1993, **115**, 6382−6390.

5   N. Robertson, *Angew. Chem. Int. Ed.*, 2006, **45**, 2338–2345.

6   F. Gao, Y. Wang, D. Shi, J. Zhang, M. Wang, X. Jing, R. Humphry-Baker, P. Wang, S. M. Zakeeruddin and M. Grätzel, *J. Am. Chem. Soc.*, 2008, **130**, 10720−10728.

7   G. C. Vougioukalakis1, M. Konstantakou, E. K. Pefkianakis, A. N. Kabanakis, T. Stergiopoulos, A. G. Kontos, A. K. Andreopoulou, J. K. Kallitsis and P. Falaras, *Asian J. Organ. Chem.*, 2014, **3**, 953–962.

8   N. M. Reddy, T. Y. Pan, Y. C. Rajan, B. C. Guo, C. M. Lan, E. W. G. Diau and C. Y. Yeh, *Phys. Chem. Chem. Phys.*, 2013, **15**, 8409–8415.

9   X. F. Wang and H. Tamiaki, *Energy Environ. Sci.*, 2010, 3, 94–106.

10   A. Yella, H. W. Lee, H. N. Tsao, C. Yi, A. K. Chandiran, Md. K. Nazeeruddin, E. W. G. Diau, C. Y. Yeh, S. M. Zakeeruddin and M. Grätzel, *Science*, 2011, **334**, 629−634.

11   J. F. Lu, X. B. Xu, K. Cao, J. Cui, Y. B. Zhang, Y. Shen, X. B. Shi, L. S. Liao, Y. B. Cheng and M. K. Wang, *J. Mater. Chem. A*, 2013, **1**, 10008−10015.

12   S. Mathew, A. Yella, P. Gao, R. Humphry-Baker, B. F. E. Curchod, N. Ashari-Astani, I. Tavernelli, U. Rothlisberger, Md. K. Nazeeruddin and M. Grätzel, *Nature Chemistry*, 2014, **6**, 242−247.

13   G. Zhang, H. Bala, Y. Cheng, D. Shi, X. Lv, Q. Yu and P. Wang, *Chem. Commun.*, 2009, 2198−2200.

14   Z. Ning, Y. Fu and H. Tian, *Energy Environ. Sci.*, 2010, **3**, 1170−1181.

15   Y. Z. Wu, M. Marszalek, S. M. Zakeeruddin, Q. Zhang, H. Tian, M. Grätzel and W. H. Zhu, *Energy Environ. Sci.*, 2012, **5**, 8261−8272.

16   J. H. Yum, T. W. Holcombe, Y. Kim, K. Rakstys, T. Moehl, J. Teuscher, J. H. Delcamp, M. K. Nazeeruddin and M. Grätzel, *Scientific Reports*, 2013, **3**, 2446.

17   X. F. Zang, Z. S. Huang, H. L. Wu, Z. Iqbal, L. Y. Wang, H. Meier and D. Cao, *J. Power Sources*, 2014, **271**, 455−64.

18   L. Han, A. Islam, H. Chen, C. Malapaka, B. Chiranjeevi, S. Zhang, X. Yang and M. Yanagida, *Energy Environ. Sci.*, 2012, **5**, 6057−6060.

19   L. L. Li and E. W. G. Diau, *Chem. Soc. Rev.*, 2013, **42**, 291−304.

20   A. Yella, C. L. Mai, S. M. Zakeeruddin, S. N. Chang, C. H. Hsieh, C. Y. Yeh and M. Grätzel, *Angew. Chem.*, 2014, **126**, 3017–3021.

21   Y. Q. Wang, B. Chen, W. J. Wu, X. Li, W. H. Zhu, H. Tian and Y. S. Xie, *Angew. Chem.*, 2014, **126**, 10955–10959.

22   J. Luo, M. F. Xu, R. Z. Li, K. W. Huang, C. Y. Jiang, Q. B. Qi, W. D. Zeng, J. Zhang, C. Y. Chi, P. Wang and J. S. Wu, *J. Am. Chem. Soc.*, 2014, **136**, 265−272.

23   T. Higashinoa and H. Imahori, *Dalton Trans.*, 2015, **44**, 448–463.

24   Y. H. Jin, J. L. Hua, W. J. Wu, X. M. Ma and F. S. Meng, *Synthetic Metals*, 2008, **158**, 64–71.

25   A. Dualeh, J. H. Delcamp, M. K. Nazeeruddin and M. Grätzel, *Appl. Phys. Lett.,* 2012, **100**, 173512–173514.

26   X. F. Lu, T. Lan, Z. W. Qin, Z. -S. Wang and G. Zhou, ACS *Appl. Mater. Interfaces*, 2014, **6**, 19308–19317**.**

27   L. Han, A. Islam, H. Chen, C. Malapaka, S. Zhang, X. Yang, M. Yanagida and B. Chiranjeevi, *Energy Environ. Sci.*, 2012, **5**, 6057–6060.

28   N. C. Jeong, H. J. Son, C. Prasittichai, C. Y. Lee, R. A. Jensen, O. K. Farha and J. T. Hupp, *J. Am. Chem. Soc.*, 2012, **134**, 19820–19827.

29   M. Kimura, H. Nomoto, N. Masaki and S. Mori, *Angew Chem. Int. Ed.*, 2012, **51**, 4371–4374.

30   L. G. Wei, Y. Na, Y. L. Yang, R. Q. Fan, P. Wang and L. Li, *Phys. Chem. Chem. Phys.*, 2015, **17**, 1273–1280.

31   H. Choi, S. Kim, S. O. Kang, J. Ko, M. S. Kang, J. N. Clifford, A. Forneli, E. Palomares, Md. K. Nazeeruddin and M. Grätzel, *Angew Chem.*, 2008, **120**, 8383–8387.

32   S. H. Fan, K. Lv, H. Sun, G. Zhou and Z. S. Wang, *J. Power Sources*, 2015, **279**, 36–47.

33   X. F. Lu, Q. Y. Feng, T. Lan, G. Zhou and Z. S. Wang, *Chem. Mater.*, 2012, **24**, 3179−3187.

34   N. W. Duffy, L. M. Peter, R. M. G. Rajapakse and K. G. U. Wijayantha, *J. Phys. Chem. B*, 2000, **104**, 8916−8919.

35   G. Schlichthorl, S. Y. Huang, J. Sprague and A. J. Frank, *J. Phys. Chem. B*, 1997, **101**, 8141−8155.

36   A. Hagfeldt and M. Grätzel, *Chem. Rev.*, 1995, **95**, 49−68.

37   N. Robertson, *Angew Chem. Int. Ed.*, 2008, **47**, 1012–1014.

38   C. L. Wang, C. M. Lan, S. H. Hong, Y. F. Wang, T. Y. Pan, C. W. Chang, H. H. Kuo, M. Y. Kuo, E. W. G. Diau and C. Y. Lin, *Energy Environ. Sci.*, 2012, **5**, 6933–6940.

39   S. Koops, B. O'Regan, P. Barnes, J. Durrant, *J. Am. Chem. Soc.*, 2009, **131**, 4808–4818.

40   J. N. Clifford, E. Martínez-Ferrerob and E. Palomares, *J. Mater. Chem.*, 2012, **22**, 12415–12422.

41   A. Hagfeldt and M. Grätzel, *Chem. Rev.*, 1995, **95**, 49−68.

42   B. C. O'Regan, K. Bakker, J. Kroeze , H. Smit, P. Sommeling, J. R. Durrant, *J. Phys. Chem. B*, 2006, **110**, 17155–17160.

43   J. N. Clifford, A. Forneli, H. Chen, T. Torres, S. Tan and E. Palomares, *J. Mater. Chem.*, 2011, **21**, 1693–1696.

44   C. M. Lan, H. P. Wu, T. Y. Pan, C. W. Chang, W. S. Chao, C. T. Chen, C. L. Wang, C. Y. Lin and E. W. G. Diau, *Energy Environ. Sci.*, 2012, **5**, 6460−6464.

45   H. P. Wu, Z. W. Ou, T. Y. Pan, C. M. Lan, W. K. Huang, H. W. Lee, N. Masi Reddy, C. T. Chen, W. S. Chao, C. Y. Yeh and E. W. G. Diau, *Energy Environ. Sci.*, 2012, **5**, 9843–9848.